

## Cryogenic vacuum issues affecting mirrors of future gravitational wave observatories

L. SPALLINO(\*)

*LNF-INFN - Via Enrico Fermi 54, 00044 Frascati, Italy*

received 31 January 2022

**Summary.** — The use of cryogenic mirrors in future gravitational wave detectors will reduce thermal noise, thus improving their sensitivity especially in the low-frequency detection range. However, when operating at cryogenic temperatures, an ice layer (“frost”) will form on the mirrors’ surface, perturbing or even preventing detection. Frost formation can be reduced but not avoided. Then, to preserve the unquestionable improvements expected by cooling down the mirrors at cryogenic temperatures, a series of necessary solutions have to be adopted. In this paper, after introducing a simple way to estimate the ice growth on the mirrors, potential mitigation methods to cure frost formation will be analysed and compared. Particular emphasis will be given to the use of electrons to induce ice desorption. Such defrost method will clearly cause electrostatic charging, which has already been shown to affect gravitational wave detection on running interferometers. Here we show that electrons not only can induce ice desorption, but can also mitigate charging issues by properly tuning their kinetic energy.

### 1. – Introduction

Five years ago, the first observations of gravitational waves (GW) caused an unprecedented and long desired scientific revolution [1]. LIGO and Virgo have made possible this extraordinary scientific enterprise, putting in place an exceptional technological effort for the interferometers’ development. Going beyond the second-generation GW detectors, scientists are now pursuing the challenge of obtaining more than 20 times higher sensitivity detectors and in a wider frequency band (spanning from  $\sim 1$  to  $\sim 10^4$  Hz). A strong research and development effort is mandatory to tackle non-trivial technological challenges to meet such scientific purposes. To this end, Einstein Telescope (ET) in Europe has been conceived so as to achieve the desired total sensitivity by using both a high

---

(\*) E-mail: [luisa.spallino@lnf.infn.it](mailto:luisa.spallino@lnf.infn.it)

frequency (at room temperature) and a low frequency (LF, at cryogenic temperature) detectors, all embedded in the overall ET layout [2].

The best conditions for detectors' sensitivity are gained only if all noises are mitigated. Thermal noise is one of the most severe limitations to low-frequency sensitivity [3]. It is due to random displacements of the mirror surfaces in response to thermally fluctuating stresses in the mirror coatings, substrates and suspensions. Since its power spectral density (to which a GW detector is sensitive) is proportional to  $T^{1/2}$  [4], cooling test masses at cryogenic temperature is an essential condition to reach the required sensitivity for LF-ET detectors.

This approach has already been foreseen at the KAGRA detector, currently under commissioning in Japan [5-7]. KAGRA recent experience is fundamental to understand the impact and the issues linked to the use of cryogenics in GW detection. Among others, when operating at cryogenic temperature, an ice layer ("frost") will inevitably form on the mirrors' surface. Ice formation is induced by molecules both residual in the mirror vessel and moving from the warm laser beam transfer line. As a consequence, as the ice layer grows, the mirror optical properties will deteriorate, perturbing or even preventing GW detection. It has been shown that, due to ice growth, the cryocooled mirrors at KAGRA GW detector undergo both a decrease in reflectivity [8-10] and an increase in thermal noise [11]. In particular, already after  $\approx 100$  nm of ice grown on the surface, reflectivity oscillations occur. These reflectivity variations induce a steady decrease of the circulating laser power in the interferometer (oscillating as reflectivity does), with a significant impact on the detector sensitivity. Estimations on power absorption induced by the ice overlayer for KAGRA have evidenced that few tens of nm of ice adlayer can absorb enough power to generate an additional heat load to the test masses, equivalent to the available thermal budget. Estimations for the LF-ET detectors are even more worrying. Already  $\sim 1$  nm of ice coverage can absorb more than the 100 mW cooling budget predicted to keep the mirrors at the foreseen temperature of 10 K. Such increase of power absorption is significant, since it indicates that a growing layer (even at nm scale) will induce more and more heat load on the test masses and drift their temperature in an uncontrolled way.

All these effects deserve further studies. However, with respect to the unquestionable improvements expected to derive by cooling down the mirrors at cryogenic temperature, such consequences, so as estimated, seem devastating and could vanish all the necessary effort to implement the use of cryogenics in the complex design of future GW detectors. An intense research and development effort is urgent to properly control and opportunely mitigate the unwanted frost formation.

Here a simple analysis is given on the way one can estimate the ice growth layer on the mirrors. The potential methods to passively or actively mitigate such ice growth will be summarised, with special attention to Electron Stimulated Desorption (ESD) very recently proposed as an active strategy to desorb ice layers on mirrors [12]. It will also be shown that, although electron irradiation can induce detrimental charging on the mirror's dielectric surface, opportunely tuning the electron energy, it is also possible to neutralize positive and negative charges induced by ESD [13].

## 2. – Frost formation

The main sources of contaminants that can be adsorbed to the mirror surface derive from the residual gas content of the Ultra High Vacuum (UHV) chamber, where the mirror is placed, and from the gas drifting from the room temperature tube of the

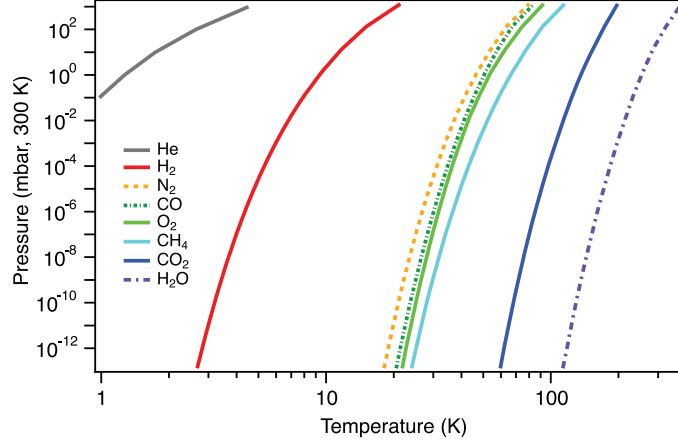


Fig. 1. – Saturated vapour pressure curves of some of the most common gasses composing the residual vacuum of a UHV system [14].

interferometer along with the laser radiation. Let us first analyse the type and quantities of gases one needs to consider.

Residual gas in vacuum will be physisorbed onto the surface depending on the gas species, on the surface temperature and on pressure values. To understand what types of gasses will be forming the adlayer on the mirrors, one can look at fig. 1 reporting the saturated vapor pressures curves of the most common gasses composing the residual vacuum of a clean UHV system [14]. The saturated vapor pressure of a single gas species is the pressure of this gas over its liquid or its solid phase, *i.e.*, the  $P$ - $T$  values at which a gas is condensed as multilayer. From fig. 1 it can be seen that, below  $\sim 30$  K, the saturated vapour pressures of most of the gases is below  $10^{-12}$  mbar. Then, if mirror surface temperature is below  $\sim 30$  K, such gases will be cryosorbed on it. If the mirror surface is at temperatures between  $\sim 30$  and 125 K, only water ice will eventually grow on it. It can be deduced that rather than the total number of molecules contained in the vacuum system (*i.e.*, the total pressure) one should be interested in the number of specific molecules contained in the vacuum system (*i.e.*, partial pressures).

Gas specific partial pressures can be measured with a calibrated Quadrupole Mass Spectrometer (QMS) [15] by Residual Gas Analysis (RGA). This gives the percentage composition of the species contributing to the total pressure. There is no universal relation between the total pressure value and the single gas composition, since the detailed composition of the residual gas depends on various aspects such as, for example, the pumping conditions and the vessel's vacuum history. To better understand this last point, in fig. 2, as an example, the RGA of a clean UHV chamber is reported, before and after a thermal treatment. This procedure, usually called bake-out, consists in heating all the chamber surfaces at a temperature as high as possible (in the range between 100 to 400 °C) for a long period (typically going from 24 h to few days) during standard pump down. By doing so, molecules adsorbed at room temperature on the vessel surfaces can be desorbed and pumped away by the active pumping system. This will improve the overall vacuum conditions.

As seen in fig. 2 (red curve), the residual gas composition of an unbaked vacuum system ( $p_T \approx 4 \times 10^{-8}$  mbar) is dominated by water. After baking the vacuum chamber

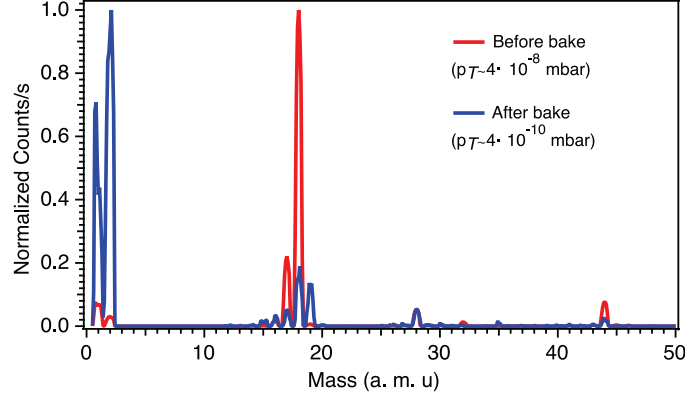


Fig. 2. – Residual gas analysis, as measured with a QMS, in case of a UHV chamber prior (red line) and after (blue line) a bake-out at 150 °C for  $\sim 48$  h. Both curves are normalized to their respective maximum.

at 150 °C (blue curve) for about 48 h, the  $\text{H}_2\text{O}$  content is strongly reduced. The bake-out not only reduces the base pressure ( $p_T \approx 4 \times 10^{-10}$  mbar), but also modifies the residual gas composition so that hydrogen becomes the dominant species.

Partial pressures inside a system which is not baked but is pumped by a large cryo-system (being it composed by cryo-pumps or cryo-panels) requires a separate analysis. Each system will behave according to their specific design, but one can expect that the partial pressures of gasses like  $\text{H}_2\text{O}$ ,  $\text{CO}$ ,  $\text{CO}_2$ ,  $\text{N}_2$ , etc., will be more similar to the ones in a well baked vessel than in an unbaked one. In UHV chambers with such a diffused cryopump system we may expect that the total pressure will be dominated by hydrogen and other gasses will each contribute only to some percent to it.

Once one has carefully considered partial pressures of all the gas species that can be cryosorbed on the mirror surface, it is fundamental to evaluate the time it will take to develop a detrimental overlayer. To this end, it is useful to introduce the Langmuir (L) as a practical unit for the gas exposure of a surface (or dosage). The Langmuir is defined by multiplying the pressure of the gas (in Torr) by the exposure time [16], so that

$$(1) \quad 1 \text{ L} = 10^{-6} \text{ Torr} \cdot 1 \text{ s}$$

Assuming that every gas molecule hitting the surface sticks to it (that is, the sticking coefficient  $S_c = 1$ ), one Langmuir (1 L) leads to a coverage of about one monolayer (ML) of the adsorbed gas molecules on the surface [16]. In general, the sticking coefficient varies depending on the temperature and on the reactivity between surface and gas particles, so that the Langmuir gives a lower limit of the time it needs to completely cover a surface with a monolayer.

All these information can be fundamental since, as better explained in the following, the proper knowledge and control of cryogenic vacuum conditions are crucial to properly limit the ice growth.

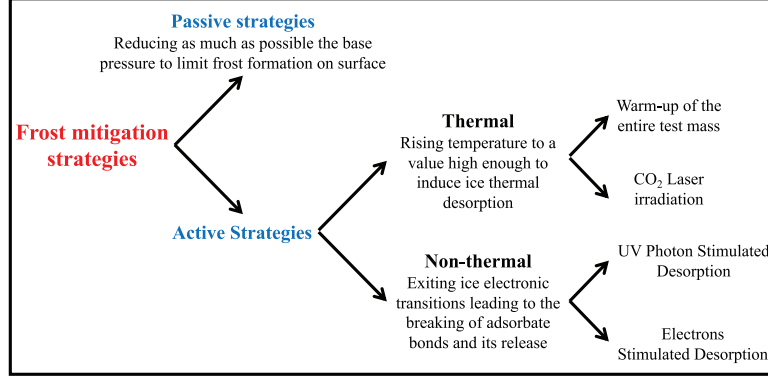


Fig. 3. – Scheme synthesising the possible methods to avoid and/or mitigate frost formation on the cryogenic mirrors' surface. More on this topic can be found in [12].

### 3. – Mitigation strategies

The time to affect the mirror properties depends on the detailed vacuum composition of the tower, but also on the vacuum seen by the mirror during cooling down and, inevitably, on the gas flow from the room temperature high conductivity vacuum tubes to the cold surfaces. It is clear that the growth of the unwanted adlayer on mirrors must be avoided and/or efficiently mitigated. This is certainly a hard challenge, requiring the full compatibility of all vacuum solutions with the maintenance of a very complex device. Mitigation strategies for removing contaminant frost from optics are currently under study, but a final strategy is still far to be decided. Hereafter, a brief overview of the possible mitigation methods by now proposed will be presented, together with some issues related to their feasibility and implementation. A synopsis is given by the scheme reported in fig. 3. An exhaustive and more complete discussion can be found in [12].

Two types of strategies are envisaged, passive and active ones.

**3.1. Passive strategies.** – Passive strategies aim to reduce the pressure in the mirror vacuum chamber and the gas flow from the long room temperature beam pipes: the lower is the pressure, the longer will take to develop an unacceptably thick ice layer. Preliminary estimates for the LF-ET mirror chambers proposed a total residual pressure of the order of  $\sim 1 \times 10^{10}$  mbar [2]. This base pressure needs to be reconsidered and reduced by carefully considering the acceptable frost allowed to develop on the mirror's surfaces in a given time. Using the notions given in the previous section, a rough estimation can be given.

At the temperature ( $T \sim 10$  K) and total pressure expected for the LF-ET mirrors, several gasses will condense on the cold mirror (see fig. 1). To be in line with the case discussed by Hasegawa and co-workers [9], let us suppose that water is one of the main species in the residual vacuum (*i.e.*,  $p_{tot} \sim p_{H_2O} \sim 1 \times 10^{10}$  mbar, where 1 mbar  $\sim 0.75$  Torr) and that  $S_c = 1$ . From eq. (1), 1 ML of water will condense on the surface in  $\sim 10^4$  s (about 3 hours). Being the thickness of 1 ML of water of the order of 0.3 nm [17], 1 nm ( $\sim 3$  ML) of ice on surface will form in  $\sim 9$  h. Following the estimations given by Tanioka *et al.* [10], about 1 nm of ice would already exceed the maximum thermal budget allowed for LF-ET. If the vacuum conditions are significantly improved so as, for

example,  $p_{\text{H}_2\text{O}} \sim 1 \times 10^{12}$  mbar, the time necessary to form 3 ML of water will be of the order of 1 month. This reasoning holds not only for water, but for all gases that sticks on a 10 K surface.

This pressure must be reached before the mirrors goes below  $T \sim 125$  K, otherwise the mirror will adsorb a thick layer during cool down. This notion implies a severe control not only on the final base pressure but also on the way and time it will be reached. Also, some limitations are needed for residual gas reaching the mirrors from the warm beam pipes. Already at the actual stage, the beamline has a stringent vacuum requirement ( $p_T \leq 10^{10}$  mbar and hydrocarbon contents  $\leq 10^{12}$  mbar to avoid laser beam absorption and scattering by the gas residual [2]). The beamlines will therefore be produced with low degassing materials and most probably baked. Nevertheless, it may be necessary to insert a so called “cold to room” temperature transition beampipe (*i.e.*, the last part of the otherwise room temperature beam pipe connecting the beam transfer line to the mirror’s vessel), with additional pumping speed to insulate the two vacuum systems.

Reducing the pressure in the UHV chamber containing the mirrors is, by itself, a great technological challenge. The same can be said for the design of the cold to warm vacuum transition. There is indeed a complex tradeoff between the desired low pressure and its costs and feasibility. Despite all efforts, however, frost will inevitably form in any case. Active strategies are therefore mandatory to remove the cryosorbed ice.

**3.2. Active strategies.** – Active methods can be implemented to desorb frost from the mirrors’ surface, both thermally and non-thermally.

**3.2.1. Thermal methods.** Thermal activated processes consist in bringing the cold test mass or its surface to a temperature high enough to induce thermal desorption (for water, above  $T \sim 125$  K). Remove frost by heating the test mass means to operate a thermal cycle of the entire system (from  $T \sim 10$  K to  $T \geq 125$  K and *vice versa*). Designing a cooling system for a suspended mass of up to 200 kg that allows fast temperature cycling is extremely challenging and expensive. Any mirror warm-up cycle may require a long down time period reducing, in an unacceptable way, the operational time of the observatories (for present designs, up to 3 months of shut down every 3 months of activity [11]).

A possible solution [10] is to illuminate the cryogenic mirror surface with a CO<sub>2</sub> laser. By stimulating molecular vibrations, CO<sub>2</sub> laser irradiation will heat the overlayer and therefore will desorb ice from the mirror surface. The recooling period may be improved in respect to heating the entire system. Still, rising the surface temperature above  $\sim 125$  K with CO<sub>2</sub> laser light will certainly induce some heat ups of the cold mass, extra thermal desorption and thermal flow. These effects must be carefully studied. Moreover, since photons will penetrate tens of  $\mu\text{m}$  into the surface, the effect of high-power photons on mirror quality must be carefully addressed. CO<sub>2</sub> laser beam could be prone to induce defects centres in the optical coatings, detrimentally influencing mirror optical quality. Also this aspect requires careful investigations.

**3.2.2. Non-thermal methods.** Non-thermal methods induce desorption by delivering to the ice enough energy to break physisorption bonds, irradiating the ice with UV photons or with electrons. These processes are known as UV Photon and Electron Stimulated Desorption (UV-PSD and ESD, respectively). UV photons can stimulate electronic transitions in molecular ice. Once stimulated, these electronic excitations can follow different relaxation pathways, one being molecular desorption. For ESD, when electrons with energy in the sub-keV range, penetrate into a surface covered with a cryosorbed ice layer, they interact with the molecules through inelastic collisions. Losing

energy, they can cause electronic excitations and molecules ionizations. Then, with an initial process similar to UV photons (electronic transitions), impinging electrons can induce molecular ice desorption.

A discussion on both these methods to remove frost in future GW detector has been made only very recently [12]. Moreover, UV photons are known to damage the test mass reflective coatings and increase laser absorption [18,19]. Due to the very high capability of UV photons to penetrate into materials ( $\sim \mu\text{m}$  [20]), it is very difficult to conceive a way to remove the ice layer and, at the same time, protect the optical quality during UV irradiation.

On the other hand, due to their very low mean free path (of the order of 1 nm, for electrons energies in the range between 10 and 1000 eV [21]), electrons do not significantly penetrate below the surface, so that minimal effects on mirror quality are expected when bombarding with electrons. However, electrons are known to induce charging effects on an insulating surface, being this latter a mirror surface or an ice layer on it. Surface charging is already a limiting noise source for GW interferometers, affecting the overall efficiency of GW detectors [22,23]. Within the LIGO collaboration, a mitigation method has been successfully applied [22,24-26]. This method implies mirror long exposure ( $\approx 1$  h) to some tenth of mbar of  $\text{N}_2$  plasma and is inapplicable (as it is now) at cryogenic temperatures. Indeed, at such low temperatures, a significant layer of  $\text{N}_2$  will be cryosorbed on the mirror surface, with the dramatic consequences discussed above. Then, in absence of a different method to mitigate charging effects in a cryogenic vacuum environment, surface charge on the GW mirror is a severe limit for using electrons to mitigate the frost growth. To this end, a new solution has been recently proposed [13] that is fully compliant with the cryogenic vacuum constraints. It is based on the ability of low-energy (between 10 to 100 eV) electrons to induce charges of both polarity on an insulating surface and, then, to neutralize charged mirrors. If this method is proved to be applicable in real GW detectors, it opens the possibility of using electrons also to mitigate ice growth on mirror surfaces.

#### 4. – Electron stimulated desorption

The discharging method mentioned above is the base to conceive ESD as a potential solution to remove the ice from the mirrors. Therefore, before giving some more quantitative details on ESD and on its advantages, the basic principles to neutralize surface charge with electrons will be presented. A complete analysis and discussion on this topic can be found in [13].

**4.1. Surface charging neutralization by low-energy electron irradiation.** – The parameter quantitatively defining the electron interaction with a material surface is the Secondary Electron Yield (SEY or  $\delta$ ). SEY is defined as the ratio between the number of all emitted electrons and incident electrons (also called primary electrons). It is experimentally determined as  $\text{SEY} = I_{\text{out}}/I_{\text{in}}$ , where  $I_{\text{in}}$  is the current of a primary electron beam hitting the surface and  $I_{\text{out}}$  is the electron current emerging from the surface [21].

At the Material Science Laboratory of the LNF, SEY is routinely measured as described in detail in refs. [13,21,27-33]. Briefly, the sample is irradiated by an electron beam emitted by a Kimball Physics electron gun equipped with a standard Ta disc cathode. SEY is performed at normal incidence and is determined by measuring, with a precision amperometer,  $I_{\text{in}}$  and the sample drain current to ground ( $I_{\text{s}}$ ).  $I_{\text{in}}$  and  $I_{\text{s}}$  are measured independently, putting alternatively the sample or a Faraday collector in



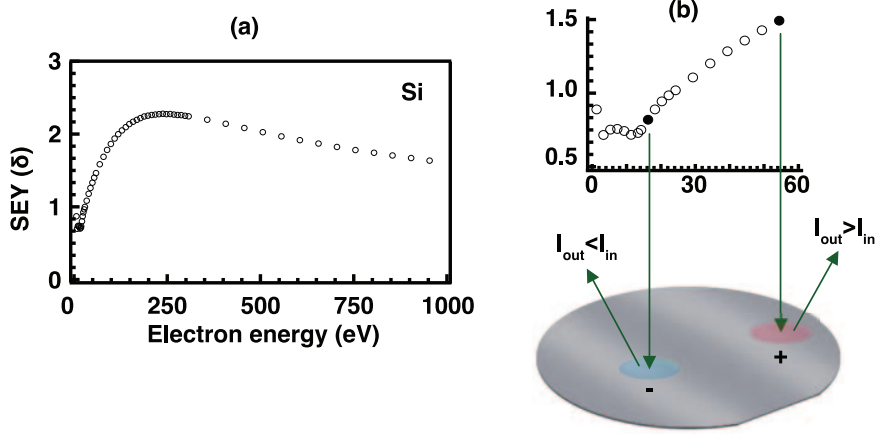


Fig. 4. – (a) SEY curves from a Si sample. (b) The graph shows the low energy part (0–60 eV) of the spectrum on the left. The arrows indicate two possible ways to induce charge on the Si surface: if surface irradiation occurs within an energy range for which  $SEY \leq 1$  (i.e.,  $I_{out} \leq I_{in}$ ), a negative charge will be delivered on the surface (sketched as a blue circle on the Si wafer); if electron irradiation occurs within an energy range for which  $SEY \geq 1$  (i.e.,  $I_{out} \geq I_{in}$ ), a positive charge will be left on the surface (sketched as a red circle).

front of the electron gun. In fact, being  $I_{out} = I_{in} - I_s$ , SEY can be expressed as  $SEY = 1 - (I_s/I_{in})$ . To measure  $I_{in}$ , the Faraday cup collector is positively biased ( $V_B = +75$  V) to prevent backscattered reemission to vacuum and, then, collect all electrons incident on it. A negative bias voltage  $V_B = -75$  V is applied to the sample to measure  $I_s$ , so as to confidently measure SEY down to low impinging electron energy (few hundreds of meV).

Figure 4(a) reports the SEY characteristics of a neutral Si substrate, here considered as representative for mirror surfaces. Depending on the primary electron energy, SEY can be  $\geq$  or  $\leq 1$  (as better evidenced on panel (b) of the figure, where a magnification of the SEY curve in the region 0–60 eV is reported). As graphically highlighted by the arrows pointing to Si surface, depending on the impinging electron energy, we can deposit electrons to the surface (at low energies, when  $SEY \leq 1$ ) or force the surface to emit more electrons than the ones deposited by the primary electron beam (at higher energies, when  $SEY > 1$ ).

This basic concept suggests the possibility to tailor electron energies to induce positive or negative charge on a neutral surface. This principle holds also in the case of an initially charged surface. Knowing the initial charge, it is always possible to opportunely tune the impinging electron energy to force the surface to eject (in case of negative charge) or to keep (in case of positive charge) electrons up to neutralization.

This method, experimentally proven in its basic aspects [13], represents a challenge requiring specific R&D on many issues to validate its implementation in the complex design of future GW detectors.

**4.2. Electrons to remove frost.** – Having access to electrons for removing ice from mirror surface has a series of advantages. As an example, let us suppose to have a  $H_2O$  layer of about 100 nm thick ( $\approx 10^{17}$  molecules/cm<sup>2</sup>) condensed on the mirror surface. Commercially available electron guns can be stably placed and immediately operated in UHV and are compatible with cryogenic environments. Typical flood guns can operate



with electron current ranging from few nA to  $\sim 20$  mA, in a spot of diameter ranging from  $\sim 10 \mu\text{m}$  to  $\sim 50$  cm. The efficiency of ESD is given by the ESD yield  $\eta$ , defined as the number of desorbed molecules per incident electron. For electron energy of about 100 eV,  $\eta \sim 0.1$  for  $\text{H}_2\text{O}$  [17]. If  $20 \text{ mA/cm}^2$  of electrons at 100 eV (corresponding to  $1.2 \times 10^{17}$  electrons/s  $\text{cm}^2$ ) are delivered on the  $\text{H}_2\text{O}$  layer, the desorption process will take just about  $10 \text{ s/cm}^2$ . In the case of ET mirrors (with a diameter  $\sim 45$  cm), defrost would take about 5 hours. The use of high current, however, has to be carefully evaluated to understand the impact on thermal budget. With an incident current of  $20 \text{ mA/cm}^2$ , the power deposited will be no more than  $\sim 2 \text{ W}$ , well above the ET extractable heat power (100 mW) [2, 34, 35]. Assuming that all the incident energy is released into thermal energy, to remain below such thermal budget, a current of at most  $\sim 1 \text{ mA/cm}^2$  should be delivered. In this case, defrost would take about  $160 \text{ s/cm}^2$  ( $\sim 3$  days for the whole mirror).

Performing a fast defrost without exceeding the thermal budget is necessary. However, ESD is a non-thermal mechanism, then almost all the energy released by the incident electrons serves to stimulate desorption. Of course, phonon modes can also be excited, thus leading to a temperature increase. The actual percentage of thermal energy needs to be evaluated in detail. Anyway, in respect to thermal desorption processes (as by heating with  $\text{CO}_2$  laser irradiation), the thermal power deposited on the surface by ESD will be significantly lower.

At this stage, all these are considerations that need an intense R&D program to validate the compliance of the proposed defrost method with all the operative constraints. More on this topic can be found in [12].

## 5. – Conclusion

Ice formation is a serious bottleneck for cryogenically cooled mirrors to be used in GW detectors. It can be reduced by improving the vacuum performances, but cannot be completely eliminated. The need of active mitigation strategies has been highlighted and an overview of possible active methods to mitigate such ice formation has been given, analysing some possible advantages and disadvantages. Particular emphasis has been given to the use of electrons to efficiently remove cryosorbed molecules. Electrons are known to be very efficient in inducing non-thermal desorption of condensed molecules from a cold surface, to potentially have very low impact on optical mirror quality and on deposited heat load. The asset for using electrons to stimulate desorption is a discharging procedure to mitigate surface charging induced by electron irradiation. Very recently a charge neutralization method, compliant with the cryogenic constraints, has been proposed. It is based on the ability of electrons to induce charges of both polarity on an insulating surface and here it has been presented in its fundamental aspects. In a synergic tandem, then electrons could be used both to remove the frost from mirrors' surface of future GW detectors and to mitigate charging issues. An intense R&D activity has to be targeted to pass from the experimentally validated idea to the refinement and implementation in the real system.

\* \* \*

The author thanks R. Cimino and M. Angelucci for the support and collaboration. The author also acknowledges the DAΦNE-L team for technical assistance and K. Battes, C. Day, S. Grohmann and A. Pasqualetti for enlightening discussions.

## REFERENCES

- [1] ABBOTT B. P. *et al.*, *Phys. Rev. Lett.*, **116** (2016) 061102.
- [2] ET STEERING COMMITTEE, *ET design report update 2020*, November 2020.
- [3] AMICO P. *et al.*, *Nucl. Instrum. Methods Phys. Res., Sect. A*, **518** (2004) 240.
- [4] HARRY G. M. *et al.*, *Class. Quantum Grav.*, **19** (2002) 897.
- [5] SOMIYA K., *Class. Quantum Grav.*, **29** (2012) 124007.
- [6] ASO Y. *et al.*, *Phys. Rev. D*, **88** (2013) 043007.
- [7] AKUTSU T. *et al.*, *J. Phys.: Conf. Ser.*, **1342** (2019) 012014.
- [8] MIYOKI S. *et al.*, *Cryogenics*, **41** (2001) 415.
- [9] HASEGAWA K. *et al.*, *Phys. Rev. D*, **99** (2019) 022003.
- [10] TANIOKA S. *et al.*, *Phys. Rev. D*, **102** (2020) 022009.
- [11] STEINLECHNER J. *et al.*, *Phys. Rev. Res.*, **1** (2019) 013008.
- [12] SPALLINO L. *et al.*, *Phys. Rev. D*, **104** (2021) 062001.
- [13] SPALLINO L. *et al.*, *Phys. Rev. D*, **105** (2022) 042003.
- [14] HONIG R. E. and HOOK H. O., *RCA Rev.*, **21** (1960) 360.
- [15] DAWSON P., *Quadrupole Mass Spectrometry and Its Applications*, in *AVS Classics in Vacuum Science and Technology* (American Institute of Physics, New York) 1995.
- [16] WOODRUFF D. P., *Modern Techniques of Surface Science*, 3rd edition (Cambridge University Press, Cambridge, UK) 2016.
- [17] DUPUY R. *et al.*, *J. Appl. Phys.*, **128** (2020) 175304.
- [18] PIVAC B. *et al.*, *Vacuum*, **71** (2003) 135.
- [19] MARKOSYAN A. *et al.*, *J. Appl. Phys.*, **113** (2013) 133104.
- [20] CRUZ-DIAZ G. *et al.*, *Astron. Astrophys.*, **562** (2014) A119.
- [21] CIMINO R. and DEMMA T., *Int. J. Mod. Phys. A*, **29** (2014) 1430023.
- [22] PROKHOROV L. G. and MITROFANOV V. P., *Class. Quantum Grav.*, **27** (2010) 225014.
- [23] BUIKEMA A. *et al.*, *Phys. Rev. D*, **102** (2020) 062003.
- [24] HEWITSON M. *et al.*, *Class. Quantum Grav.*, **24** (2007) 6379.
- [25] BUCHMAN S. *et al.*, *Class. Quantum Grav.*, **25** (2008) 035004.
- [26] CAMPSIE P. *et al.*, *Class. Quantum Grav.*, **28** (2011) 215016.
- [27] CIMINO R. *et al.*, *Phys. Rev. Lett.*, **93** (2004) 014801.
- [28] CIMINO R. *et al.*, *Phys. Rev. Lett.*, **109** (2012) 064801.
- [29] CIMINO R. *et al.*, *Phys. Rev. ST Accel. Beams*, **18** (2015) 051002.
- [30] GONZALEZ L. *et al.*, *AIP Adv.*, **7** (2017) 115203.
- [31] SPALLINO L. *et al.*, *Appl. Phys. Lett.*, **114** (2019) 153103.
- [32] SPALLINO L. *et al.*, *Phys. Rev. Accel. Beams*, **23** (2020) 063201.
- [33] ANGELUCCI M. *et al.*, *Phys. Rev. Res.*, **2** (2020) 032030(R).
- [34] PUNTURO M. *et al.*, *Class. Quantum Grav.*, **27** (2010) 194002.
- [35] HILD S., *Class. Quantum Grav.*, **29** (2012) 124006.